Int. J. Electrochem. Sci., 7 **(2012)** 1677 - 1687

International Journal of
ELECTROCHEMICAL
SCIENCE
www.electrochemsci.org

Electrochemical Synthesis of Polyaniline on Nanodiamond Powder

Jianbing Zang[1,2], *Yanhui Wang*[1,*], *Xiyan Zhao*[1], *Guoxiang Xin*[1], *Shuping Sun*[1], *Xuanhui Qu*[2], *Shubing Ren*[2]

[1] State Key Laboratory of Metastable Material Science & Technology, College of Material Science & Engineering, Yanshan University, Qinhuangdao, China, 066004
[2] State Key Laboratory for Advanced Metals and Materials, School of Materials Science and Engineering, University of Science and Technology Beijing, Beijing, P.R. China, 100083
[*]E-mail: diamond_wangyanhui@163.com

Received: 26 December 2011 / *Accepted:* 18 January 2012 / *Published:* 1 February 2012

Conductive polyaniline (PANI) was electropolymerised on undoped nanodiamond (ND) powder by potentiodynamic deposition in sulphuric acid solution containing aniline monomer. The influences of anodic potential limit and concentrations of aniline monomer and H_2SO_4 on cyclic voltammetry behaviour were investigated. The results showed that PANI was deposited on the ND powder electrode under an anodic potential limit of 1.1-1.5 V. However, a high anodic potential above 1.0 V was only necessary to initiate the polymerisation in initial cycles, so PANI was further grown from −0.2 to 0.9 V to avoid overoxidation and degradation. The PANI growth rate increased with the increasing concentrations of aniline monomer and H_2SO_4, but it decreased when the monomer concentration was higher than 0.3 M. Fourier transform infrared spectrum and scanning electron microscope confirmed the presence of PANI. At the initial polymerisation, the PANI nanoparticles were deposited on the ND surfaces. The fibril PANI increased during further growth and linked the ND particles together, forming a porous network structure. The impedance of the PANI/ND electrode was far lower than that of the ND powder electrode. The composite electrode demonstrated higher conductivity and better capacitance behaviour.

Keywords: polyaniline; electropolymerise; nanodiamond; cyclic voltammetry

1. INTRODUCTION

Nanodiamond (ND) powder is becoming one of the most widely studied nanomaterials because it not only exihibits the unique properties of diamond, such as superior hardness, high chemical stability and thermal conductivity, but also possesses the features of a nano-scale material, including a giant specific surface area and large numbers of surface defects. Several potential applications for ND in biology [1-3], medicine [4, 5], and catalysis [6-8], have been reported.

Most recently, the electrochemical properties of undoped ND have attracted the attention of researchers. Detonation-synthesised undoped 5 nm diamond nanoparticles show redox behaviour in various solutions [9-11] due to the surface chemistry of the particles. They are found to greatly promote oxygen reduction reactions [12] and oxidation of nitrite anions [13]. Considering the unique properties of diamond electrodes such as wide potential window, low background current, and high chemical and electrochemical stabilities, ND is expected to be used as an electrode material in many electrochemical fields. One problem with ND is its too low conductivity. How to increase the conductivity of the ND electrode has become the focus of research, in order to expand its use in the diamond applications electrochemistry field.

Polyaniline (PANI) is a particularly interesting conducting polymer. It exhibits high conductivity in its oxidised/protonated form, possesses high environmental stability, and good electrochemical reversibility [14-17]. PANI-coated carbon-based materials have been widely investigated as electrode materials in supercapacitors owing to their good conductivity and large pseudo-capacitance [18-24]. They have also been considered as new forms of support for electrocatalysts because of their highly accessible surface area and low resistance [25]. Deposition of PANI on ND particles is expected to obtain a novel composite with a high conductivity and a high stability [26].

In this work, PANI was deposited on undoped ND powder by electrochemical cyclic voltammetry (CV) method. The effects of anodic limit potential and concentrations of aniline monomer and sulphuric acid on the CV behaviour were investigated. The electrochemical properties of the resulting composite electrode were discussed.

2. EXPERIMENTAL

The ND powders with a particle size below 100 nm, fabricated by mechanical milling, were the commercial products of Henan Boreas Technological Development Co. A ND powder electrode was prepared by filling the ND powders into a plastic pipe (0.5 mm in diameter at the tip) with no binder [26].

All the electrochemical experiments were carried out by a CHI660A electrochemistry analyser in a single compartment with a traditional three-electrode system, which consisted of a platinum coil counter electrode, an Ag/AgCl reference electrode and a ND powder or a PANI/ND composite electrode as a working electrode. PANI was electropolymerised at a ND powder electrode through CV in sulphuric acid aqueous solution. After polymerisation, the electrode was repeatedly washed with deionised water, and dried at room temperature. The powder was taken out from the plastic pipe for further characterisation. Fourier transform infrared (FTIR) spectra of the prepared PANI/ND composite in a KBr disk were recorded on an E55+FRA106 type IR spectrometer. The morphology was observed with field-emission electron microscopy (FESEM, Hitachi S4800). The composite electrode was repeatedly washed with background electrolyte (0.5 M H_2SO_4) and then placed in monomer-free background electrolyte to perform AC impedance measurements. The potential amplitude was kept at 5 mV and the frequency range was 10^{-1}-10^{5} Hz. Typical Nyquist plots of the PANI/ND composite electrode in 0.5 M H_2SO_4 solution were recorded under different potentials.

All solutions were prepared using reagent grade chemicals in deionised water.

3. RESULTS AND DISCUSSION

3.1 Effect of upper potential limit on electropolymerisation of PANI

Fig. 1 shows the progressive CVs at the ND powder electrode in 0.2 M aniline + 0.5 M H_2SO_4 with different upper potential limits at a sweep rate of 0.05 V/s. The characteristics of the CVs were similar to one another. The first cycle showed a well-defined peak corresponding to the oxidation of aniline at approximately 1.0 V, which decreased drastically in subsequent cycles. The other redox peaks (A/A′, B/B′, C/C′, D/D′) were developed and increased during the potential scanning (Fig. 1a). The redox peaks A/A′ and D/D′ were attributed to the transition of leucoemeraldine to emeraldine, and emeraldine to pernigraniline, respectively. The peaks appearing in the middle (B/B′, C/C′) corresponded to the redox of the benzoquinone/hydroquinone couple (as hydrolysis product) and/or the redox of head-to-tail dimer [27-29]. The above results suggested that a PANI film was electropolymerised on the ND powder electrode under an anodic potential limit of 1.1-1.5 V. A gradual increase in peak current values with an increase of the number of cycles confirmed the growth of the conductive PANI film. It was also found that a higher anodic potential resulted in higher peak currents, indicating a faster growth of PANI. In the literature [30], it has been mentioned that the formation of the dimer-like benzidine (tail-to-tail dimer) or *p*-aminodiphenylamine (head-to-tail dimer) during the polymerisation is enhanced at a high anodic potential, and these oligomeric radical cations can act as nuclei for further aniline polymerisation. So the application of a high anodic potential can increase the polymer growth rate by increasing the number of polymerisation nuclei.

However, faster growth of PANI would result in a more irregular structure and it would consequently be less conductive [31]. Moreover, it was also noted that the redox peaks D/D′ shifted to less positive potentials, and the oxidation peak current became relatively weaker under a higher anodic potential limit (Fig. 1b and c). Simultaneously the redox peaks A/A′ shifted in the positive direction, whilst the intensity of the middle peaks corresponding to redox of the degradation product and/or the redox of the dimer became stronger. The results suggested formation of the over-oxidised PANI and severe degradation under a high anodic potential [32-34].

On the other hand, the peak current at 1.0 V decreased quickly and disappeared in several sweeps (Fig. 1d), implying that once the cation radicals were activated in the first cycle to initiate the polymerisation, the self-catalysis of PANI controlled the further growth in the following sweeps, and the high potential of above 1.0 V was not needed any more. Further polymerisation could be carried out under an anodic potential below 1.0 V in order to avoid PANI overoxidation and degradation [35]. Fig. 2 shows the further growth of PANI at the ND powder electrode from –0.2 to 0.9 V. As expected, the middle peaks clearly decreased, suggesting less degradation of the PANI under a lower anodic potential limit.

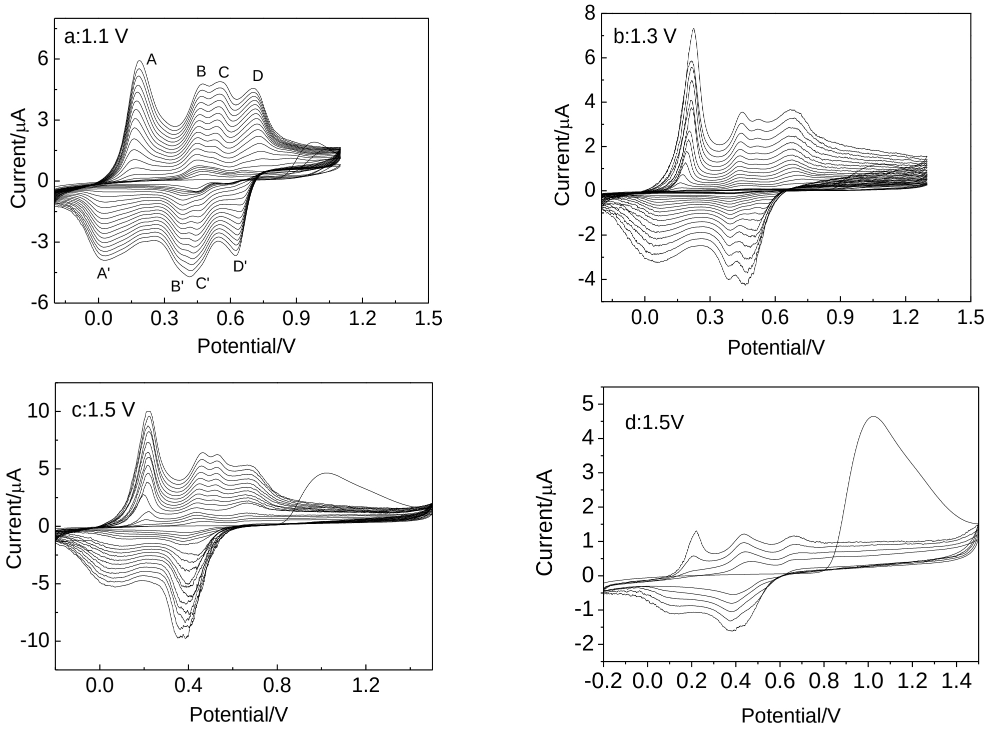

Figure 1. CV curves in 0.2 M aniline + 0.5 M H_2SO_4 at different anodic potential limits: (a) 1.1 V, (b) 1.3 V, (c) 1.5 V, (d) the initial 5 cycles of (c).

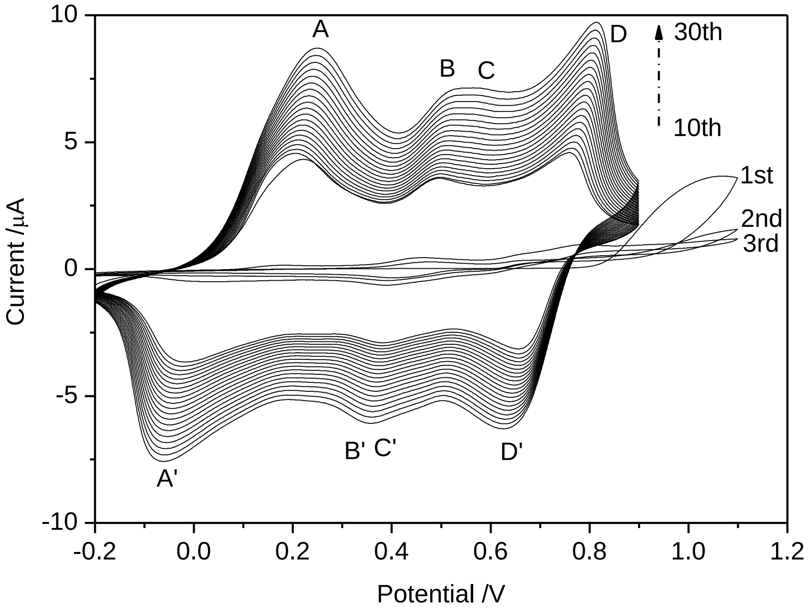

Figure 2. CV curves in 0.2 M aniline + 0.5 M H_2SO_4 from −0.2 to 0.9 V.

3.2 Effect of the concentrations of aniline monomer and H_2SO_4 supporting electrolyte

Fig. 3 presents the CVs taken at different concentrations of aniline in 0.5 M H_2SO_4 at 0.05 V/s. All CVs were obtained after initial 3 sweeps from −0.2 to 1.1 V. The development and increase in three (or four) well-defined peak pairs attributed to the formation of PANI were observed. An increase in the current intensity with increasing monomer concentration showed a higher growth rate of PANI in the solution containing more monomers. However, when the monomer concentration was higher than 0.3 M, the growth rate decreased. A much higher concentration limits the possibility of the aniline monomer reacting with radical cations due to combinative performance [36].

To study the effect of the concentration of H_2SO_4 on the polymerisation of PANI, several electrodes were prepared, keeping the concentration of aniline at 0.2 M, but varying the concentration of H_2SO_4 from 0.2 to 1.0 M. Fig. 4 shows the fifteenth cycle of CVs taken in different concentrations of H_2SO_4 electrolyte at 0.05 V/s. The growth rate of PANI increased with an increase in the acid concentration because more protons were available for the PANI redox process. The deposition of PANI was slow at low concentration of H_2SO_4 (0.1 M, as inset in Fig. 4), and the peaks merged because of the low proton availability [31, 37].

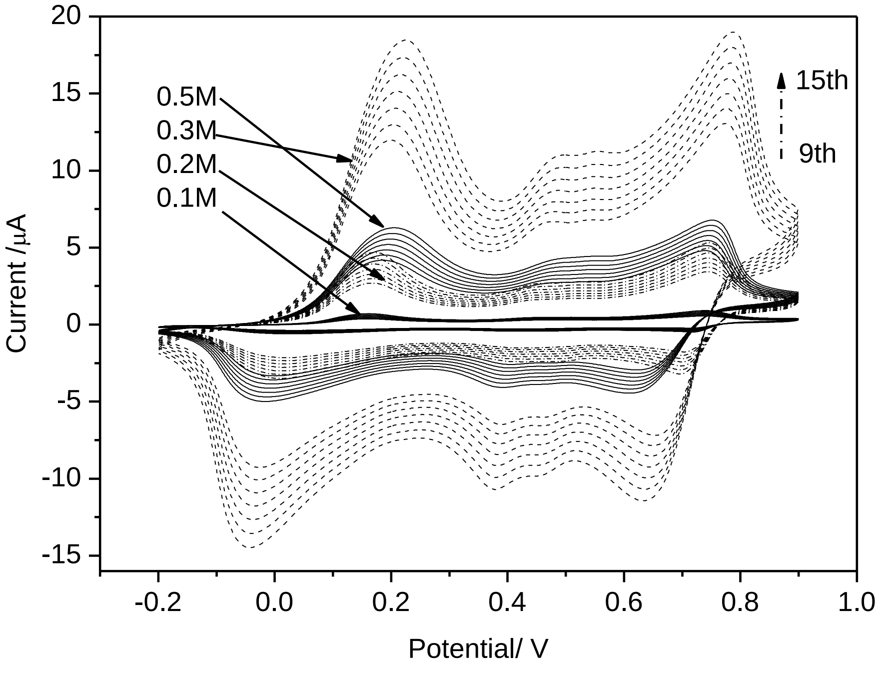

Figure 3. CV curves obtained at different aniline concentrations in 0.5 M H_2SO_4.

3.3 Microstructure of the PANI/ND composite

The FTIR spectra of the ND powder and the PANI/ND composite are shown in Fig. 5. Curve *a* shows characteristic bands of the functional groups on the surface of the ND powder. The peaks at 1733 and 1090 cm^{-1} were assigned to the modes of stretching C=O vibration and C–O vibration. The peak at 1633 cm^{-1} was attributed to deformation C–OH vibrations [38]. On curve *b*, the peaks at 1483 and 1566 cm^{-1} corresponded to quinone- and benzene ring stretching deformations, respectively, which were characteristics of PANI. The absorbance corresponding to C–N stretching, C–N$^{\cdot+}$ stretching, and –NH^{+}= stretching appeared at 1305, 1244, and 1139 cm^{-1}. The peaks at 818 and 880 cm^{-1} were assigned to C–H out of plain bending [39, 40]. The presence of all these vibrational modes clearly proved that the ND was covered by the conducting PANI film.

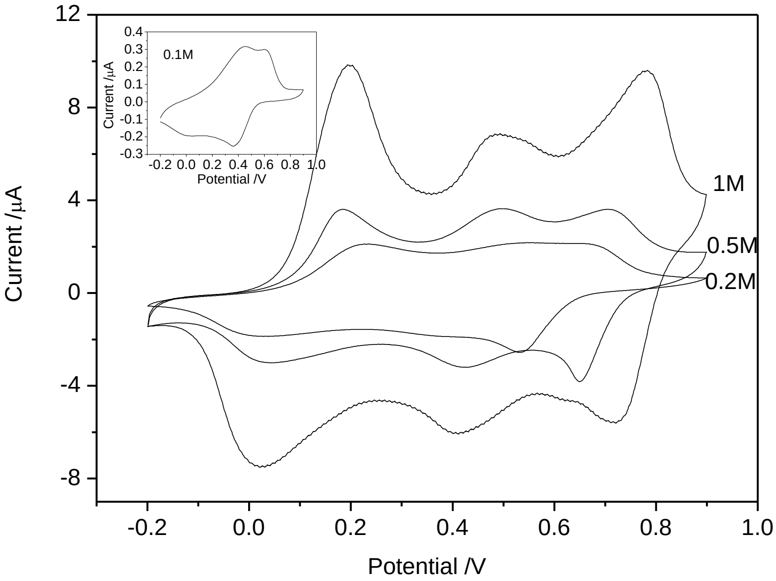

Figure 4. The fifteenth cycle of the electropolymerisation at 0.2 M aniline in different concentrations of H_2SO_4 electrolyte.

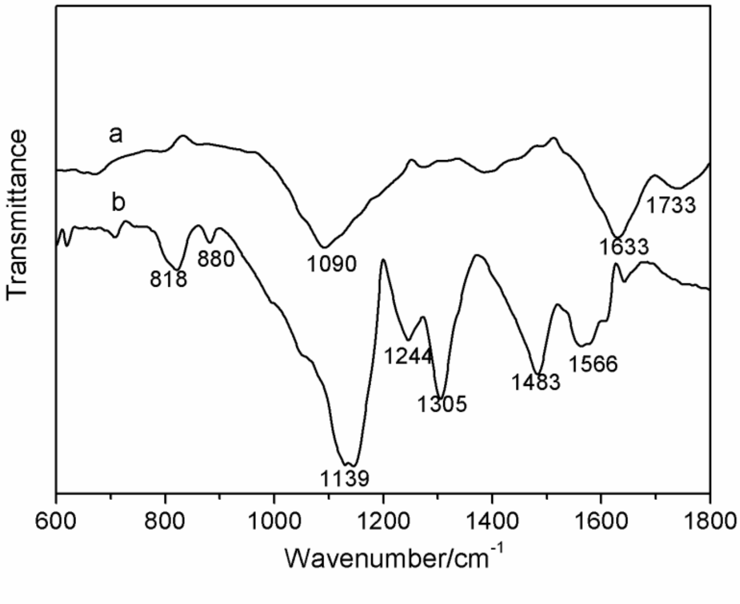

Figure 5. FTIR spectra of the pristine ND powder (a) and the PANI/ND composite prepared in 0.2 M aniline + 0.5 M H_2SO_4 for 15 cycles (b).

Fig. 6 shows the morphology of the PANI/ND composite. The pristine ND powder used in this study was fabricated by mechanical milling. As shown in Fig. 6a, the average size of ND particles was about 100 nm and the surface was smooth. It was observed that the ND particles were covered by PANI nanoparticles after electropolymerising for 5 cycles (Fig. 6b). Some PANI fibrils were also observed. The fibroid PANI increased during further growth, and linked the ND particles together, forming a porous network structure (Fig. 6c). With an increase in the number of cycles, the fibril diameter increased, and the PANI film became thicker (Fig. 6d).

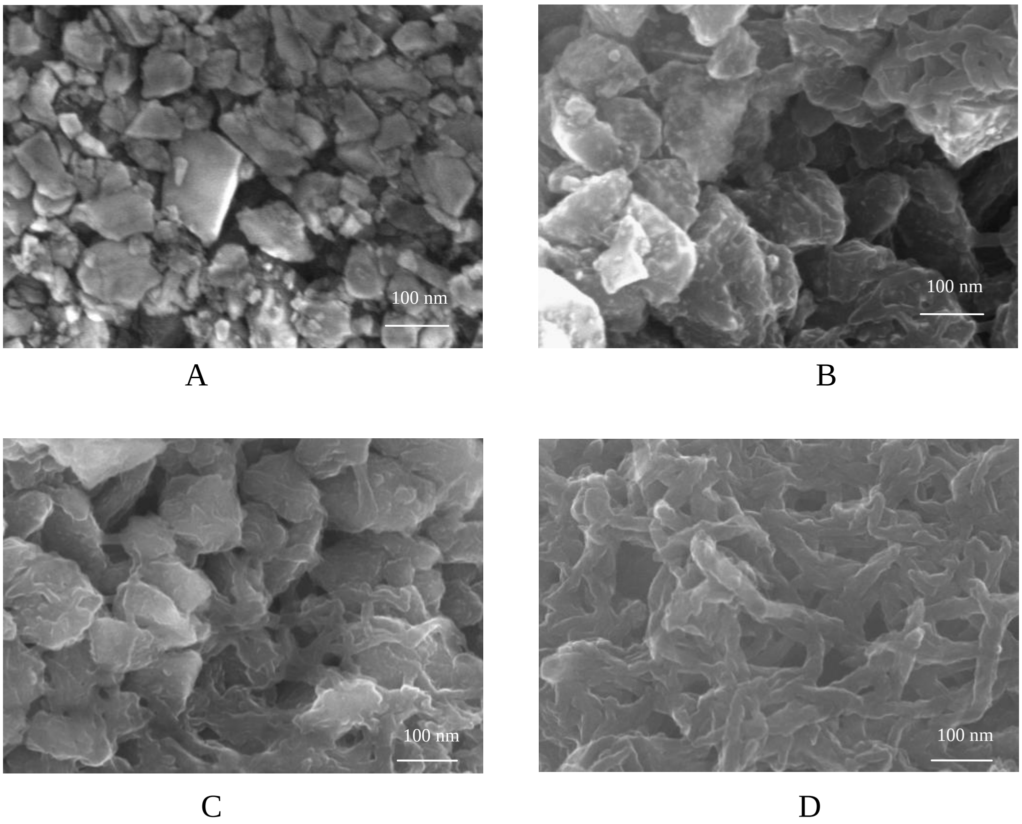

Figure 6. FESEM images of the pristine ND powder (a) and the PANI/ND composite prepared in 0.2 M aniline + 0.5 M H_2SO_4 for 5 cycles (b), 15 cycles (c), and 30 cycles (d).

The morphology of PANI is related to its mode of nucleation and growth during polymerisation [41, 42]. In this study, the PANI nanoparticles were deposited on the ND surfaces during initial polymerisation by applying a high anodic potential limit. For subsequent polymerisation, additional PANI grew in a one-dimensional structure using the pre-existing polymers as nucleation sites (secondary growth), which led to the nanofibrous PANI [43]. As the cycle numbers increased, the interconnected nanofibre networks were formed. The rough and porous morphology imparts to the PANI/ND composite a large specific surface area, which will be useful in applications as an electrocatalyst support or an electrode material in capacitors.

3.4 Impedance analyses of the resulting electrode

Electrochemical impedance spectroscopy (EIS) was employed to investigate electrochemical properties of the PANI/ND composite electrode. The oxidation structures of PANI were strongly dependent on the applied potentials, so the impedance curves of the PANI/ND electrode prepared in 0.2 M aniline + 0.5 M H_2SO_4 for 15 cycles were measured at different applied potentials in 0.5 M H_2SO_4. The Nyquist impedance plots obtained at the potentials of 0, 0.2, 0.5, and 0.7 V, respectively, are given in Fig. 7a~d. The Nyquist impedance plot of a pristine ND powder electrode at 0.5 V is also shown in Fig. 7e for purposes of comparison.

All impedance curves had a semicircle in the high-frequency region, which was attributed to the process at the polymer/electrolyte interface [28]. This can be described by the double layer capacitance in parallel with the ionic charge-transfer resistance (R_{ct}). The high-frequency intercept of the semi-circle on the real axis yielded the ohmic resistance (R_s) while the diameter provided the charge transfer resistance (R_{ct}) of the electrode/electrolyte interface. The R_{ct} value changed with the potentials as inferred from the diameter of the semicircle, attributed to the conductivity changes of different PANI structures. The minimum R_{ct} came out at 0.2-0.5 V (Figs. 7b and c) since the polymer was in conductive emeraldine (50% oxidised) state. The conversion of oxidation states from the emeraldine (50% oxidised) to the leucoemeraldine (fully reduced) form at 0 V (Fig. 7d) or to the pernigraniline (fully oxidised) form at 0.7 V (Fig. 7a) resulted in a decrease in conductivity and, consequently, an increase in charge transfer resistance.

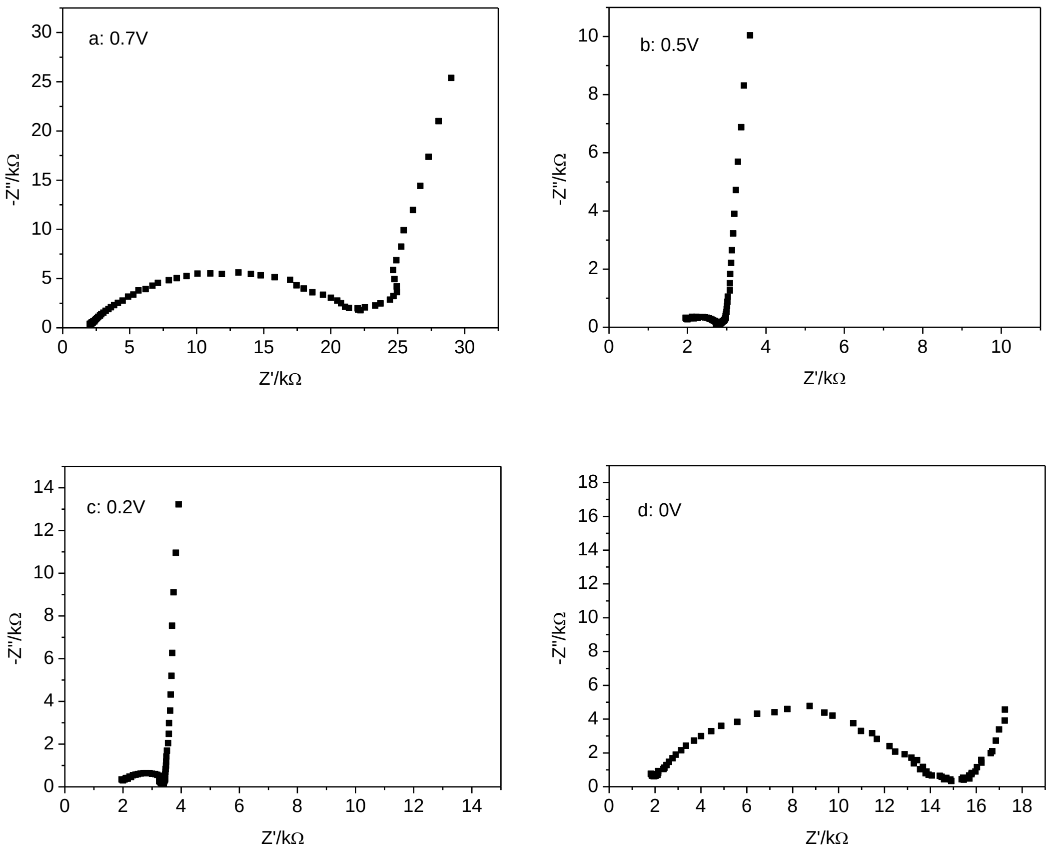

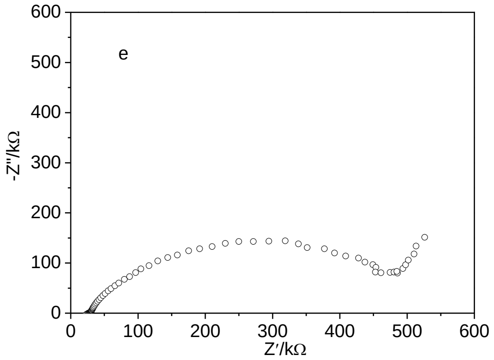

Figure 7. Nyquist impedance plots of the PANI/ND electrode at 0.7 V (a), 0.5 V (b), 0.2 V (c), 0 V (d), and the ND powder electrode at 0.5 V (e) in 0.5 M H_2SO_4.

In Figs. 7b and c, a nearly vertical line in the low-frequency region was found, suggesting an ideal capacitive behaviour, which should be attributed to the faradaic capacitance of the PANI deposited on the ND particles [28, 33]. In the whole frequency range, the impedance of the PANI/ND electrode was two orders of magnitude lower than that of pristine ND powder electrode (Fig. 7e). This suggested a significant improvement on the conductivity of the ND powders after deposition of PANI.

4. CONCLUSIONS

PANI/ND composite was fabricated by electrochemical CV under different conditions. Although a potential limit higher than 1.0 V was necessary in initial sweeps to initiate the oxidation of aniline and form radicals for further polymerisation, the subsequent growth of PANI was performed under an anodic potential below 1.0 V in order to avoid overoxidation or degradation. The growth rate of PANI increased with increasing concentrations of aniline monomer and H_2SO_4. However, when the aniline concentration was higher than 0.3 M, the growth rate decreased. FTIR confirmed the presence of PANI on the ND. The PANI nanoparticles were deposited on the ND surfaces during initial polymerisation. The fibroid PANI increased during further growth, and linked the ND particles together, forming a porous network structure. The EIS results pointed out an enhancement in the conductivity of the ND powder electrode after electrodeposition of PANI. The PANI/ND composite electrode also demonstrated better capacitance behaviour. These results suggest that the PANI/ND composite can be utilised as an electrode material in capacitors or an electrocatalyst support material.

ACKNOWLEDGMENTS

The authors gratefully acknowledge the support of the National Natural Science Foundation of China (Grant Nos. 50972125 and 50872119), Natural Science Foundation of Hebei Province (No. E2011203126), and China Postdoctoral Science Foundation (20100480197).

References

1. X.L. Kong, L.C.L. Huang, C.M. Hsu, W.H. Chen, C.C. Han, H.C. Chang, *Anal. Chem.* 77 (2005) 259.
2. X. Kong, L.C.L. Huang, S.C.V. Liau, C.C. Han, H.C. Chang, *Anal. Chem*. 77 (2005) 4273.
3. S.J. Yu, M.W. Kang, H.C. Chang, K.M. Chen, Y.C. Yu, *J. Am. Chem. Soc*. 127 (2005) 17604.
4. C.C. Fu, H.Y. Lee, K. Chen, T.S. Lim, H.Y. Wu, P.K. Lin, P.K. Wei, P.H. Tsao, H.C. Chang, W. Fann, *Proc. Natl. Acad. Sci*. U.S.A. 104 (2007) 727.
5. A.M. Schrand, H.J. Huang, C. Carlson, J.J. Schlager, E. Osawa, S.M. Hussain, L.M. Dai, *J. Phys. Chem.* B 111 (2007) 2.
6. G.P. Bogatyreva, M.A. Marinich, E.V. Ishchenko, V.L. Gvyazdovskaya, G.A. Bazalii, N.A. Oleinik, *Phys. Solid State* 46 (2004) 738.
7. Y.L. Yuan, L. Wang, X.L. Feng, *Eur. Polym. J.* 38 (2002) 2125.
8. T. Tsoncheva, V. Mavrodinova, L. Ivanova, M. Dimitrov, S. Stavrev, C. Minchev, *J. Mol. Catal*. A 259 (2006) 223.
9. J.B. Zang, Y.H. Wang, S.Z. Zhao, L.Y. Bian, J. Lu, *Diam. Relat. Mater*. 16 (2007) 16.
10. K.B. Holt, C. Ziegler, D.J. Caruana, J.B. Zang, E.J. Millán-Barrios, J.P. Hu, J.S. Foord, *Phys. Chem. Chem. Phys.* 10 (2008) 303.
11. K.B. Holt, C. Ziegler, J.B. Zang, J.Foord, J.P. Hu, *J. Phys. Chem*, 113 (2009) 2761.
12. W. Zhao, J.J. Xu, Q.Q. Qiu, H.Y. Chen, *Biosens. Bioelectron*. 22 (2006) 649.
13. L.H. Chen, J.B. Zang, Y.H. Wang, L.Y. Bian, *Electrochim. Acta* 53 (2008) 3442.
14. Y. Cao, T.E. Mallouk, *Chem. Mater*. 20 (2008) 5260.
15. G.Y. Zhao, H.L. Li, *Micropor. Mesopor. Mater*. 110 (2008) 590.
16. K. Ghanbari, M.F. Mousavi, M. Shamsipur, *Electrochim. Acta* 52 (2006) 1514.
17. M. Gerard, B.D. Malhotra, *Appl. Phys*. 5 (2005) 174.
18. W.C. Chen, T.C. Wen, *J. Power Sources* 117 (2003) 273.
19. V. Gupta, N. Miura, *Electrochim. Acta* 52 (2006) 1721.
20. E. Frackowiak, V. Khomenko, K. Jurewicz, K. Lota, F. Béguin, *J. Power Sources* 153 (2006) 413.
21. J.G. Deng , X.B. Ding, W.C. Zhang, Y.X. Peng, J.H. Wang, X.P. Long, P. Li, A.S. C. Chan, *Eur. Polym. J.* 38 (2002) 2497.
22. Y.K. Zhou, B.L. He, W.J. Zhou, J.E. Huang, X.H. Li, B. Wu, H.L. Li, *Electrochim. Acta* 49 (2004) 257.
23. L.X. Li, H.H. Song, Q.C. Zhang, J.Y. Yao, X.H. Chen, *J. Power Sources* 187 (2009) 268.
24. W. C. Chen, T. C. Wen, H. Teng. *Electrochim. Acta* 48 (2003) 641.
25. G. Wu, L. Li, J.H. Li, B.Q. Xu, *Carbon* 43 (2005) 2579.
26. X.Y. Zhao, J.B. Zang, Y.H. Wang, L.Y. Bian, J.K. Yu, *Electrochem. Commun*. 11 (2009) 1297.
27. M. Matsushita, H. Kuramitz, S. Tanaka, *Environ. Sci. Technol*. 39 (2005) 3805.
28. W.C. Chen, T.C. Wen, C.C. Hu, A. Gopalan, *Electrochim. Acta* 47 (2002) 1305.
29. P. Santhosh, K.M. Manesh, A. Gopalan, K.P. Lee, *Anal. Chim. Acta* 575 (2006) 32.
30. A.Zimmermann, U. Kinzelman, L. Dunsch, *Synthetic Met.* 93 (1998) 17.
31. S.R. Moraes, D. Huerta-Vilca, A.J. Motheo, *Eur. Polym. J*. 40 (2004) 2033.
32. S.K. Mondal, N. Munichandraiah, *J. Electroanal. Chem*. 595 (2006) 78.
33. R. Pauliukaite, C.M.A. Brett, A.P. Monkman, *Electrochim. Acta* 50 (2004) 159.
34. Y. Zhao, M. Chen, T. Xu, W. Liu, *Colloid. Surface* A 257–258 (2005) 363.
35. C. Dalmolin, S.C. Canobre, S.R. Biaggio, R.C. Rocha-Filho, N. Bocchi, *J. Electroanal. Chem*. 578 (2005) 9.
36. P. Nunziante, G. Pistoia, *Electrochim. Acta* 34 (1989) 223.
37. S.K. Mondal, K. Barai, N. Munichandraiah, *Electrochim. Acta* 52 (2007) 3258.
38. E. Mironov, A. Koretz, E. Petrov, *Diam. Related Mater*. 11 (2002) 872.
39. M. Trchová, I. Šeděnková, E. Tobolková, J. Stejskal, *Polym. Degrad. Stabil*. 86 (2004) 179.

40. M. Trchová, I. Šeděnková, J. Stejskal, *Synthetic Met*. 154 (2005) 1.
41. H.D. Tran, Y. Wang, J.M. D’Arcy, R.B. Kaner, *ACS Nano* 2 (2008) 1841.
42. D. Li, R.B. Kaner, *J. Am. Chem. Soc.* 128 (2006) 968.
43. Y. Guo, Y. Zhou, *Eur. Polym. J.* 43 (2007) 2292.